

Electronic supplementary information

Na₂Fe₂F₇ Fluoride-based Cathode for High Power and Long Life Na-Ion Batteries

Hyunyoung Park^{a,1}, Yongseok Lee^{a,1}, Min-kyung Cho^b, Jungmin Kang^a, Wonseok Ko^a, Young Hwa Jung^c, Tae-Yeol Jeon^c, Jihyum Hong^d, Hyungsub Kim^e, Seung-Taek Myung^{a,}, and Jongsoon Kim^{a,*}*

Corresponding Authors: Prof. Seung-Taek Myung (smyung@sejong.ac.kr), Prof. Jongsoon Kim (jongsoonkim@sejong.ac.kr).

^a Department of Nanotechnology and Advanced Materials Engineering, Sejong University, Seoul, 05006, Republic of Korea

^b Advanced Analysis Center, Korea Institute of Science and Technology (KIST), Seoul, 02792, Republic of Korea

^c Beamline Division, Pohang Accelerator Laboratory (PAL), Pohang, 37673, Republic of Korea

^d Center for Energy Materials Research, Korea Institute of Science and Technology (KIST), Seoul, 02792, Republic of Korea

^e Korea Atomic Energy Research Institute (KAERI), Daedeok-daero 989 Beon-Gil, Yuseong-gu, Daejeon, 34057, Republic of Korea

¹ H.P. and Y. L. contributed equally to this work.

Experimental

Preparation of T-Na₂Fe₂F₇

We carefully prepared 1.428 g of NaF (99%, Alfa Aesar), 1.613 g of FeF₂ (98%, Sigma Aldrich), and 1.959 g of FeF₃ (97%, Alfa Aesar) based on stoichiometry of Na₂Fe₂F₇ composition. The precursors were sealed in a silicon nitride jar in an Ar-filled glove box, and they were mixed by high-energy ball milling at 400 rpm for 12 h. The mixed powder was pelletized and heated to 650 °C for 30 min under an Ar gas flow. Before the experiment, Super P and carbon nanotubes (CNTs) were also mixed by high-energy ball milling at 150 rpm for 12 h to enhance the electrical conductivity.

Electrochemical characterization

The T-Na₂Fe₂F₇ electrode was prepared by mixing the active material, Super P as the conducting carbon, and poly(vinylidene fluoride) (PVDF) as the binder using *N*-methyl-2-pyrrolidone (NMP) as the solvent. A slurry (70 wt% active materials, 19 wt% Super P, 1 wt% CNTs, and 10 wt% PVDF) was applied to Al foil using a doctor blade. The electrode was dried in a vacuum oven at 80 °C for 12 h to evaporate the NMP. The mass loading of the electrode was ~2 mg cm⁻².

R2032-type coin cells were prepared using the T-Na₂Fe₂F₇ electrode, Na metal as the reference/counter electrode, a separator (Whatman GF/F glass fiber), and 0.5 M NaPF₆ in propylene carbonate (PC): fluoroethylene carbonate (FEC) (volume ratio of 98:2) as the electrolyte. The PC solvent and 0.5 M NaPF₆ were chosen because they can provide stable cycle performance along with high ionic conductivity.^{1,2} In addition, the reason on application of 0.5 M NaPF₆ electrolyte for this study is due to the limited solubility of NaPF₆ in propylene carbonate (PC) and fluorinated ethylene carbonate (FEC) solution. It was reported that over 0.5

M NaPF₆ salts were not perfectly dissolved in PC : FEC solution.³ Furthermore, applying 0.5 M NaPF₆ based electrolyte for the NIB system were reported at various research papers, which is another reason on adaptation of 0.5 M NaPF₆ electrolyte for this study.⁴⁻⁶ The coin cells were assembled in an Ar-filled glove box.

Galvanostatic charge/discharge tests were performed at various current rates (C/20, C/10, C/5, C/2, 1C, 2C and 5C in the voltage range of 1.5–4.3 V (vs. Na⁺/Na); charge current density fixed at C/20) using a battery test system (WonATech WBCS3000). Additionally, galvanostatic intermittent titration technique (GITT) measurement was conducted. A current rate of C/20 was applied for 30 min at each charge/discharge step, followed by a 10 min relaxation step in the voltage range of 1.5–4.3 V (vs. Na⁺/Na). In this experiment, 1C corresponds to ~184 mA g⁻¹.

X-ray diffraction

T-Na₂Fe₂F₇ was analyzed using XRD (Malvern Panalytical Empyrean) using Cu K α radiation ($\lambda = 1.54178 \text{ \AA}$). The step size was 0.13°, and the 2 θ range of 10°–80° was examined. *Operando* synchrotron XRD (*o*-SXRD) analyses were performed at beamline 3D of the Pohang Accelerator Laboratory (PAL) to investigate the structural evolution during charge/discharge at a current rate of C/8 in the voltage range of 1.5–4.3 V (vs. Na⁺/Na). The *o*-SXRD patterns were collected using synchrotron radiation ($\lambda = 0.688725 \text{ \AA}$) with a Mar345 image plate detector in transmission mode and an X-ray exposure time of 5 s. After the measurement, the 2 θ angles of all the *o*-SXRD patterns were recalculated to the corresponding angles for $\lambda = 1.54178 \text{ \AA}$, which is the wavelength of a conventional X-ray tube source with Cu K α radiation, for ease of comparison with other published studies. Rietveld refinement of the XRD and *o*-SXRD data and bond-valence energy landscape (BVEL) analysis were performed using the FullProf software package.⁷

Scanning electron microscopy

The morphology and particle size of T-Na₂Fe₂F₇ were determined using scanning electron microscopy (SEM; Hitachi SU-8010), operated at 15 keV. Before the measurement, each specimen was coated with Pt nanoparticles to enhance the conductivity.

Field-emission transmission electron microscopy

The morphology and particle size of T-Na₂Fe₂F₇ were determined and energy-dispersive X-ray spectroscopy (EDS) elemental mapping was performed using field-emission transmission electron microscopy (FE-TEM; JEOL JEM-F200), operated at 300 keV. Before the measurement, the T-Na₂Fe₂F₇ powder was sonicated in ethanol, and droplets of the suspension were spread onto a carbon-coated Cu TEM grid. The specimen was dried at room temperature overnight to evaporate the ethanol.

High-resolution transmission electron microscopy

High-resolution particle images of T-Na_xFe₂F₇ ($1 \leq x \leq 3$) were obtained and the d-spacings with SAED patterns were determined using high-resolution transmission electron microscopy (HR-TEM; FEI TITAN 80-300), operated at 300 keV. The available point resolution is better than 1 Å at an operating accelerating voltage. Each image was recorded by a 4k × 4k CCD camera (Gatan Oneview1095). Electron energy loss (EEL) spectra were collected using a Gatan Quantum 966 spectrometer. Before the measurement, each specimen was sonicated in ethanol, and droplets of the suspension were spread onto a carbon-coated Cu TEM grid. It was dried at room temperature overnight to evaporate the ethanol.

Inductively coupled plasma optical emission spectrometry

The atomic ratios of elements (Na and Fe) were determined using inductively coupled plasma-optical emission spectrometry (ICP-OES; Thermo ICAP-6000).

XAS

Ex-situ X-ray absorption spectroscopy (XAS) spectra for the Fe K-edge (in the energy range of 6930–7930 eV) were obtained at beamline 6D at PAL. Each specimen was prepared in the form of an electrode, and Fe metal foil was used as a reference. The collected XAS data were analyzed using Athena software.⁸

Fabrication of full cell

Full cells were fabricated using commercial hard carbon (Kureha) as the anode. The hard carbon was heated at 1000 °C for 2 h under an Ar gas flow to remove residual water and the air-oxidized substance on the surface of the hard carbon particles. The hard carbon electrode was fabricated in the same way and using the same ratio as for the T-Na₂Fe₂F₇ electrode except that Cu foil was used. To minimize the irreversibility of hard carbon, the hard carbon electrode was pre-cycled as a half cell through direct contact with Na metal in the range of 0.01–2.0 V at 40 mA g⁻¹. Finally, R2032-type full cells were assembled with the T-Na₂Fe₂F₇ cathode and hard carbon anode (capacity ratio of negative and positive electrodes of ~1.2) in an Ar-filled glove box.

Computational details

All the density functional theory (DFT) calculations were performed using the Vienna Ab initio Simulation Package (VASP).⁹ We used projector-augmented wave (PAW) pseudopotentials¹⁰ with a plane-wave basis set as implemented in VASP. Perdew–Burke–Ernzerhof (PBE) parametrization of the generalized gradient approximation (GGA)¹¹ was used for the exchange-correlation functional. For the DFT calculations, a $5 \times 5 \times 2$ k-point grid was used to calculate a $1 \times 1 \times 1$ supercell structure of T-Na₂Fe₂F₇. The GGA+U method¹² was adopted to address the localization of the d-orbital in Fe ions, with a U value of

5.0 eV, as determined in a previous report.^{13,14} An appropriate number of k-points and a kinetic energy cutoff of 500 eV were used in all the calculations. All the structures were optimized until the force in the unit cell converged to within 0.03 eV Å⁻¹.

NEB calculations¹⁵ were performed to determine the activation barrier for Na diffusion in the T-Na₂Fe₂F₇ structure. To perform the calculations, five intermediate images were generated between each Na site. These structures were then calculated using the NEB algorithm with fixed lattice parameters and free internal atomic positions.

The schematic illustrations, crystal structure with BVOL, and NEB calculation results for Na⁺ diffusion pathways were drawn using VESTA software.¹⁶

Supplementary Figures

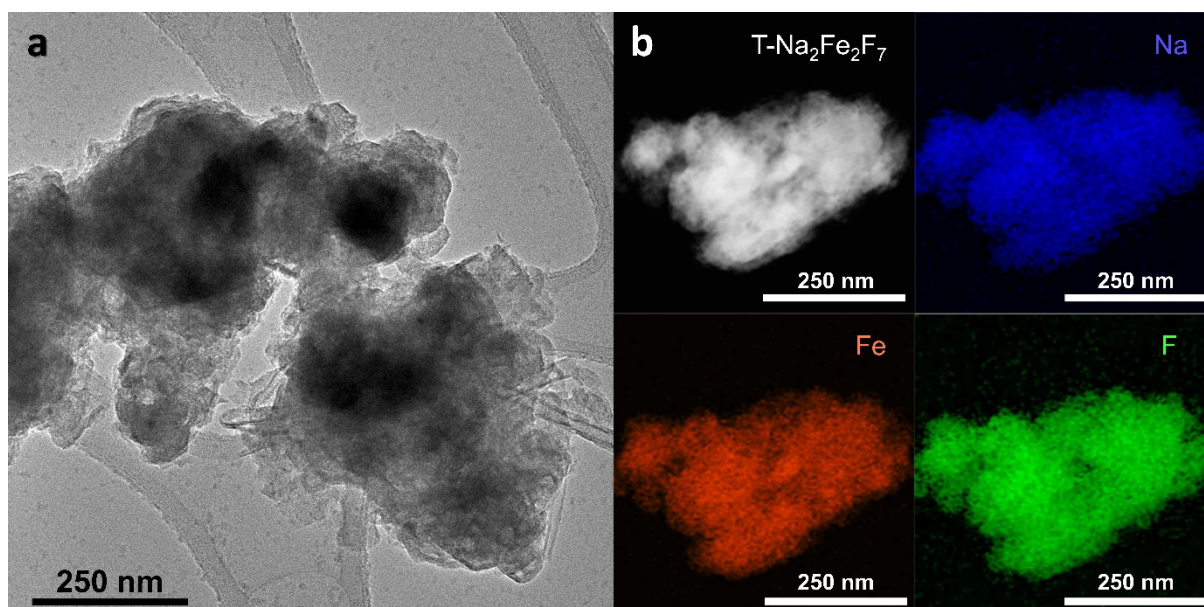


Fig. S1 (a) TEM image and (b) EDS elemental mappings of T-Na₂Fe₂F₇.

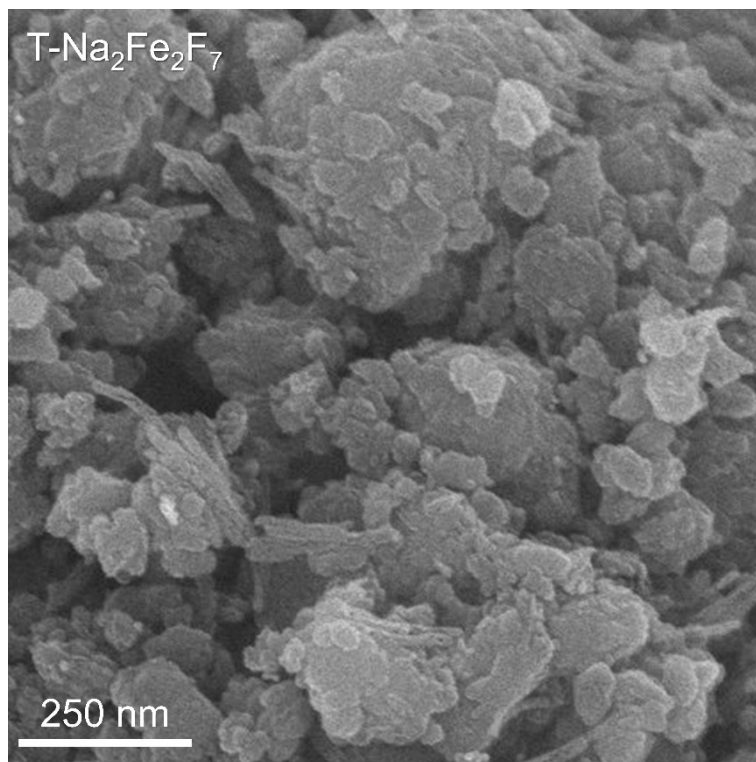


Fig. S2 SEM image of T- $\text{Na}_2\text{Fe}_2\text{F}_7$.

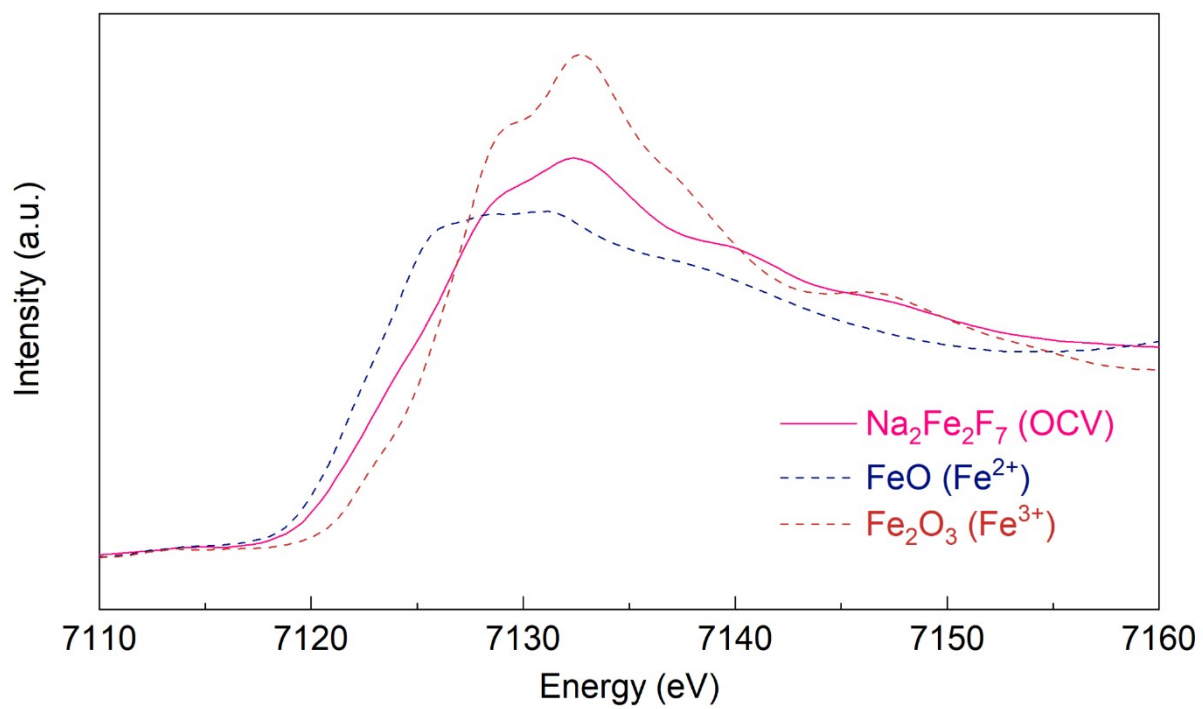


Fig. S3 K-edge XANES spectra of T-Na₂Fe₂F₇.

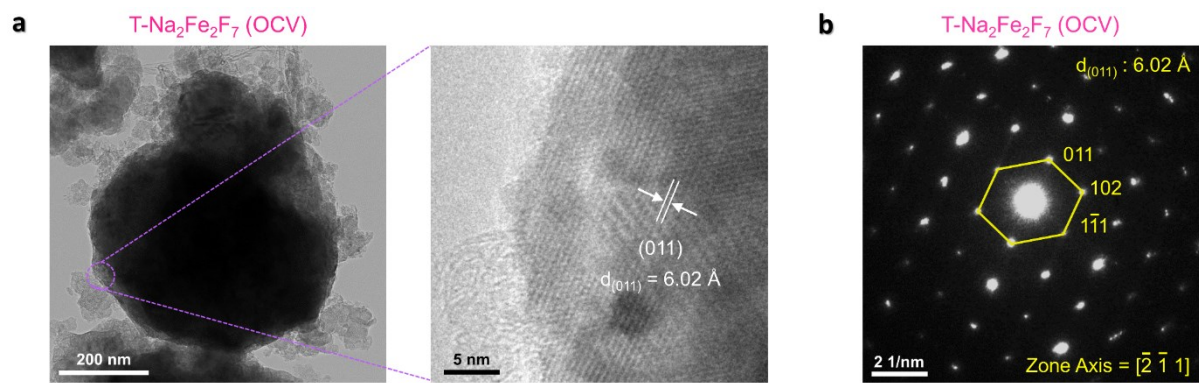


Fig. S4 (a) TEM image and magnified view with (b) SAED pattern of T-Na₂Fe₂F₇.

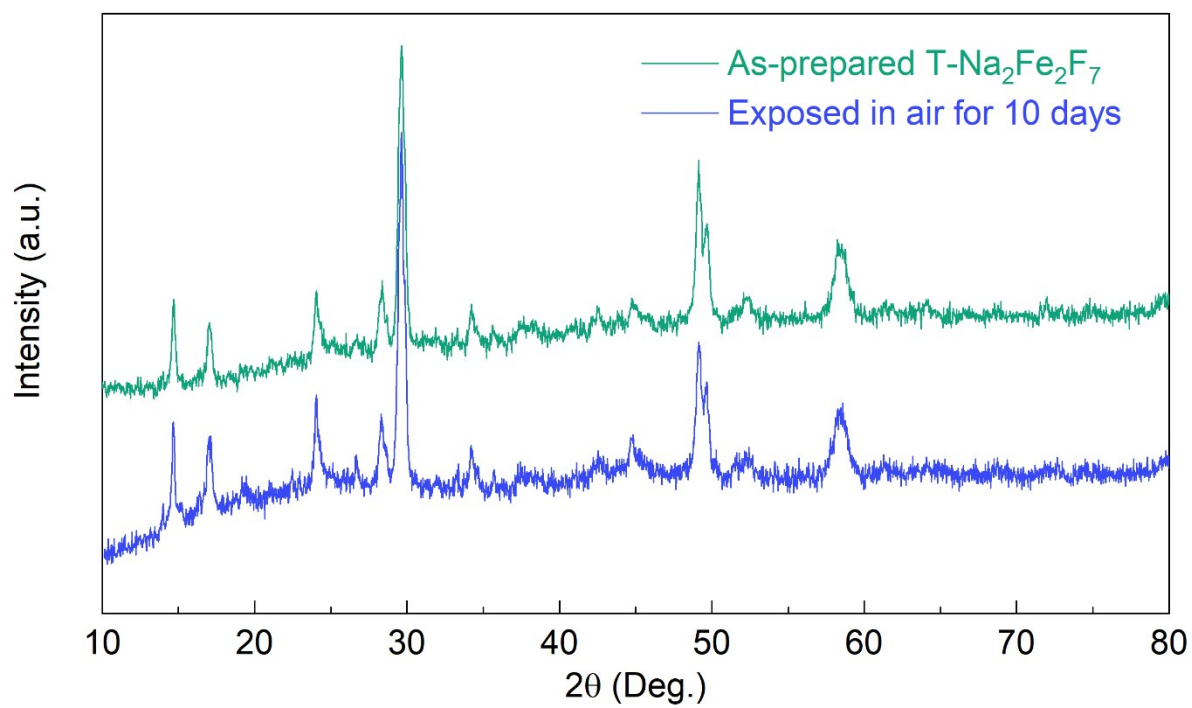


Fig. S5 XRD patterns of T-Na₂Fe₂F₇ exposed to air for 10 days.

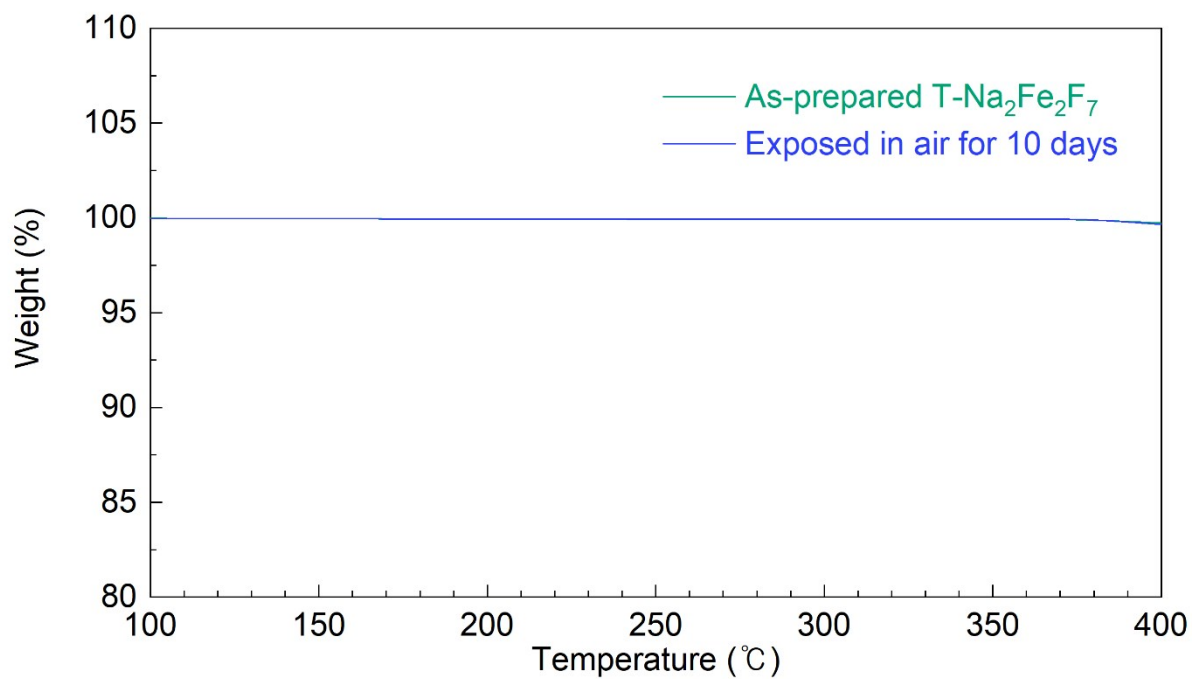


Fig. S6 TGA analyses of T-Na₂Fe₂F₇ exposed to air for 10 days.

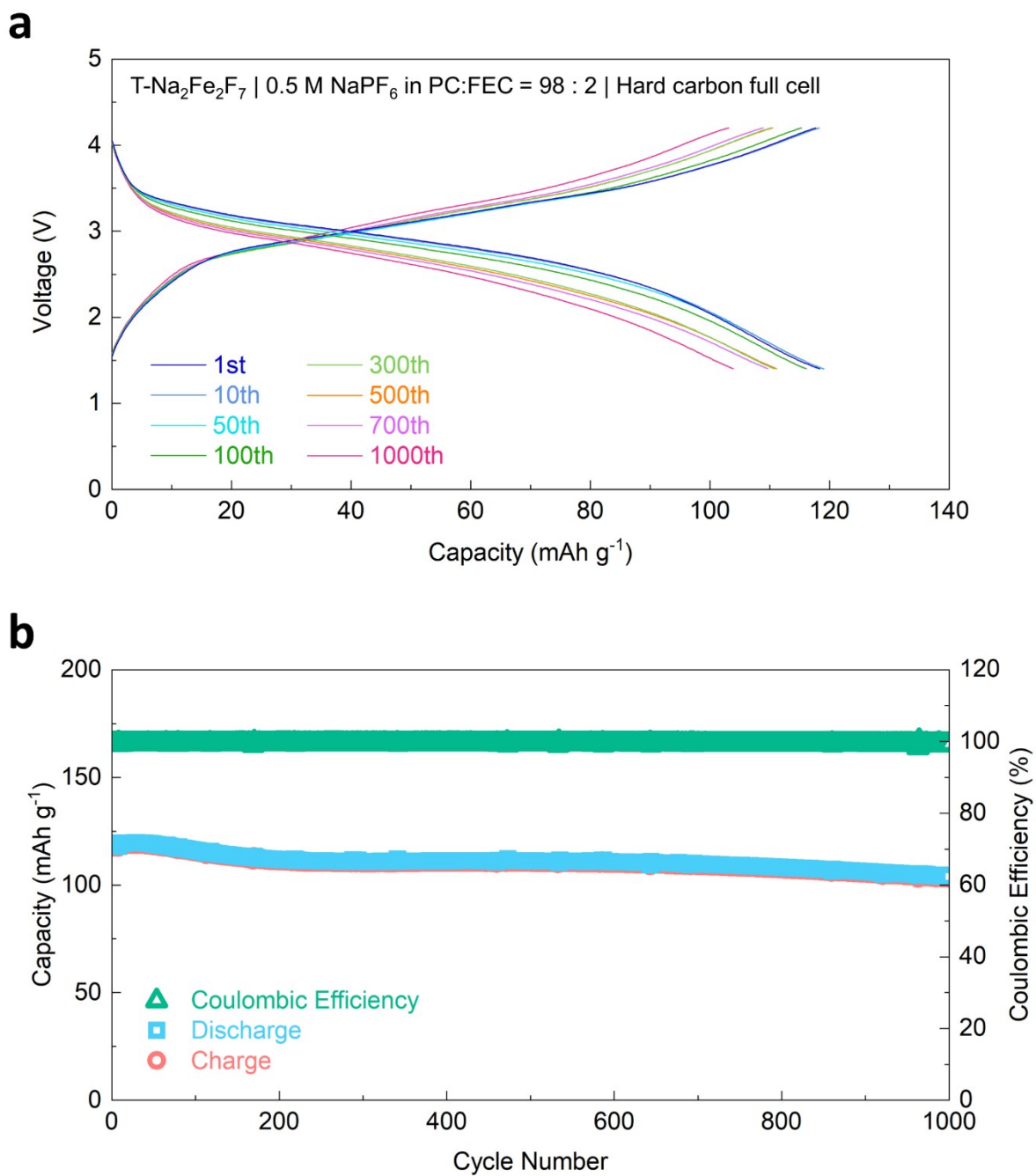


Fig. S7 (a and b) (a) Charge/discharge curves and (b) cycling performance of T- $\text{Na}_2\text{Fe}_2\text{F}_7$ // hard carbon full cell at 368 mA g^{-1} over 1000 cycles.

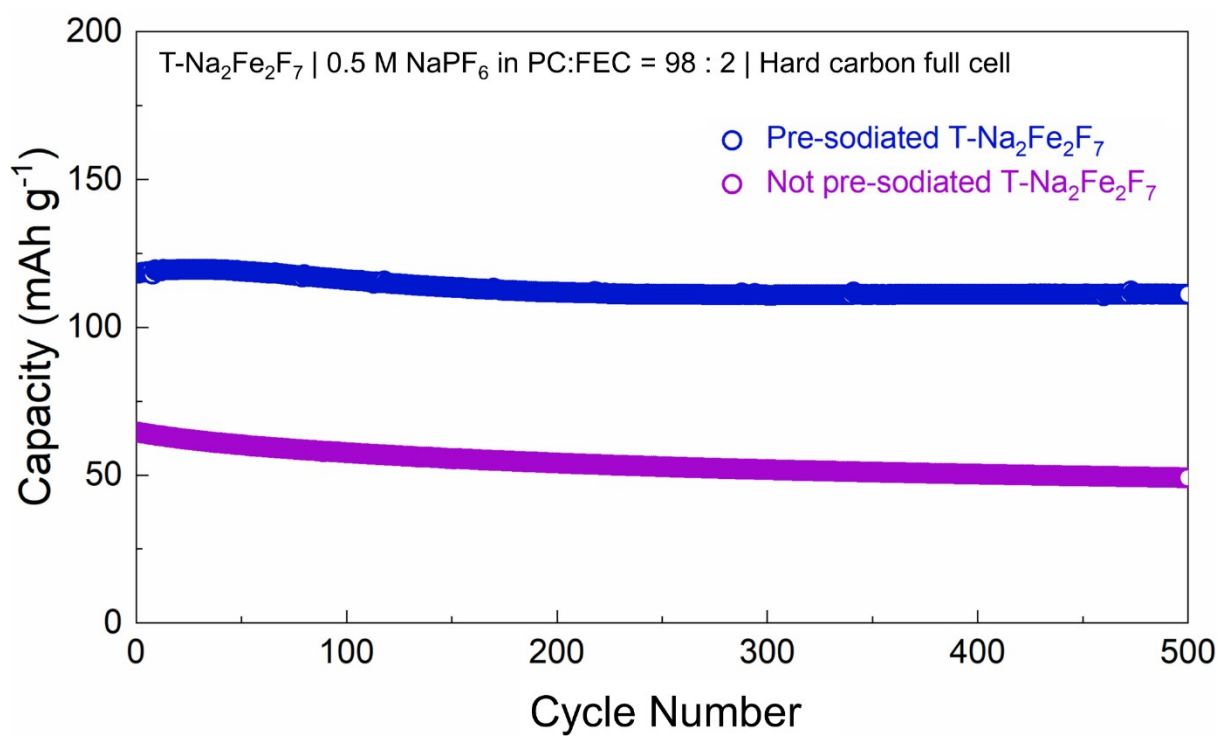


Fig. S8 Cycling performance of T-Na₂Fe₂F₇ // hard carbon full cell at 368 mA g⁻¹ with or without pre-sodiation of T-Na₂Fe₂F₇ cathode.

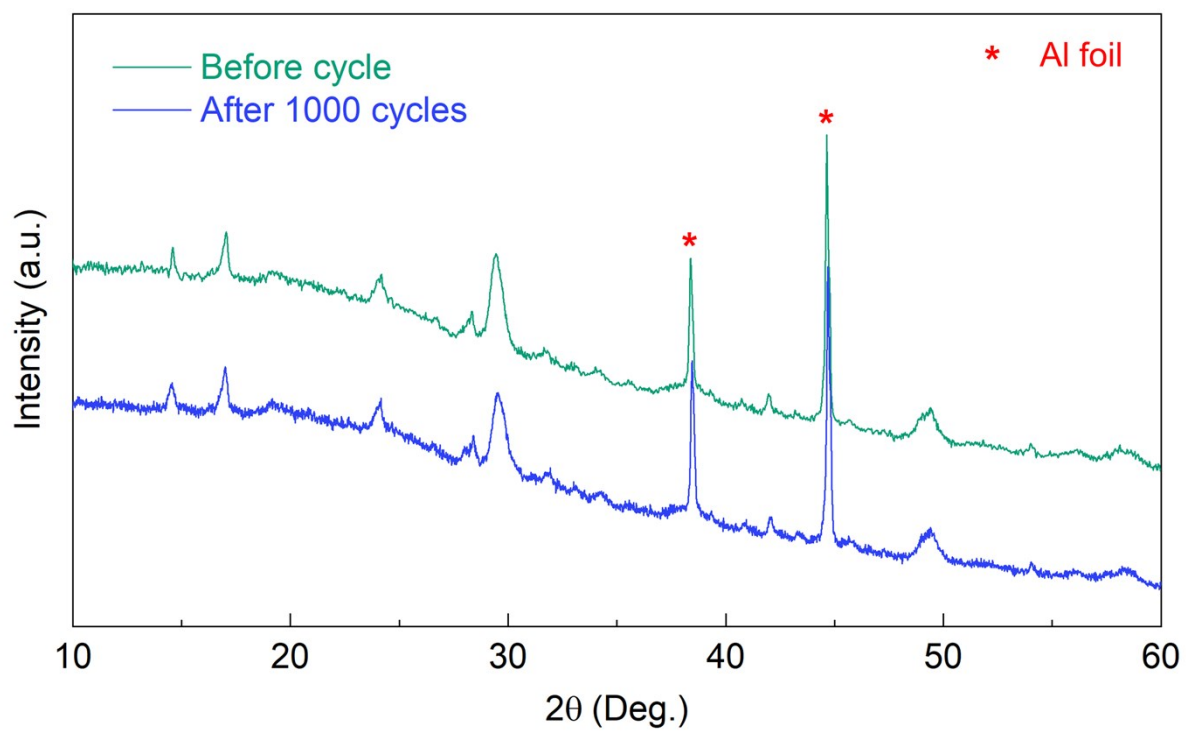


Fig. S9 *Ex-situ* XRD patterns of T-Na_xFe₂F₇ before and after cycling for 1000 cycles.

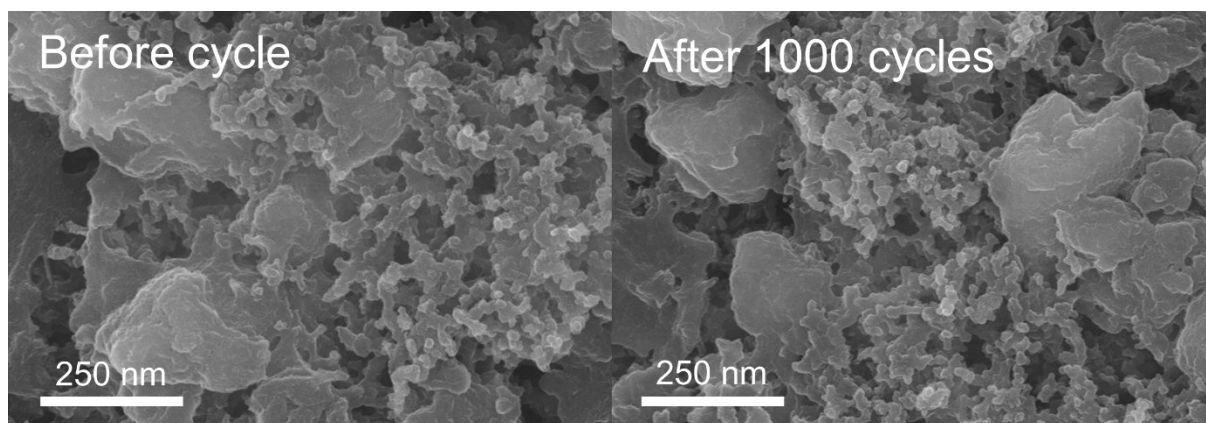


Fig. S10 Magnified SEM images of T-Na_xFe₂F₇ electrode before and after cycling for 1000 cycles.

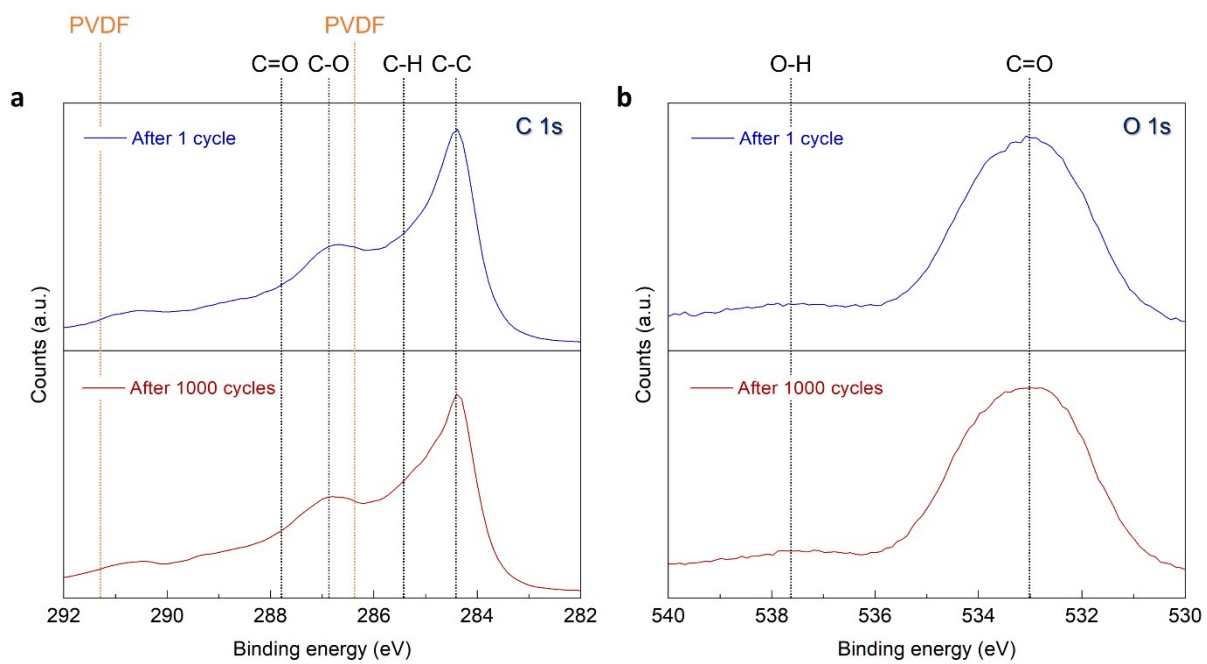


Fig. S11 XPS spectra of T-Na_xFe₂F₇ after 1000 cycle: (a) C 1s peaks and (b) O 1s peaks.

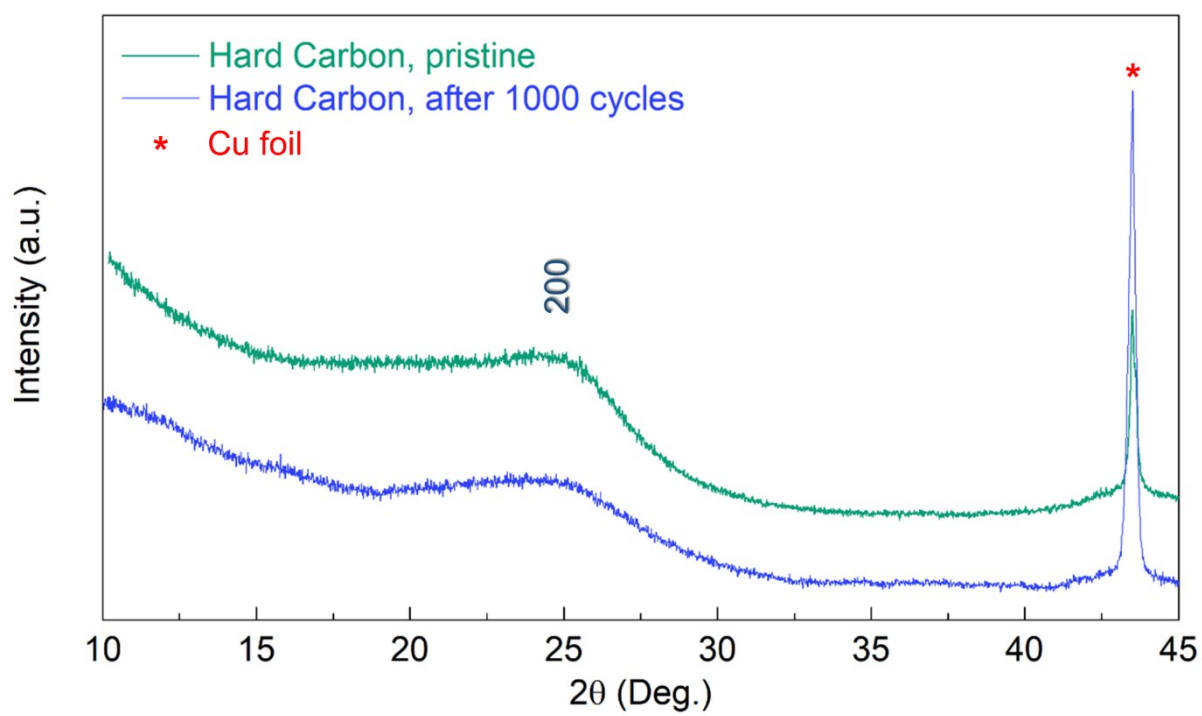


Fig. S12 XRD analyses of hard carbon electrode after cycling for 1000 cycles.

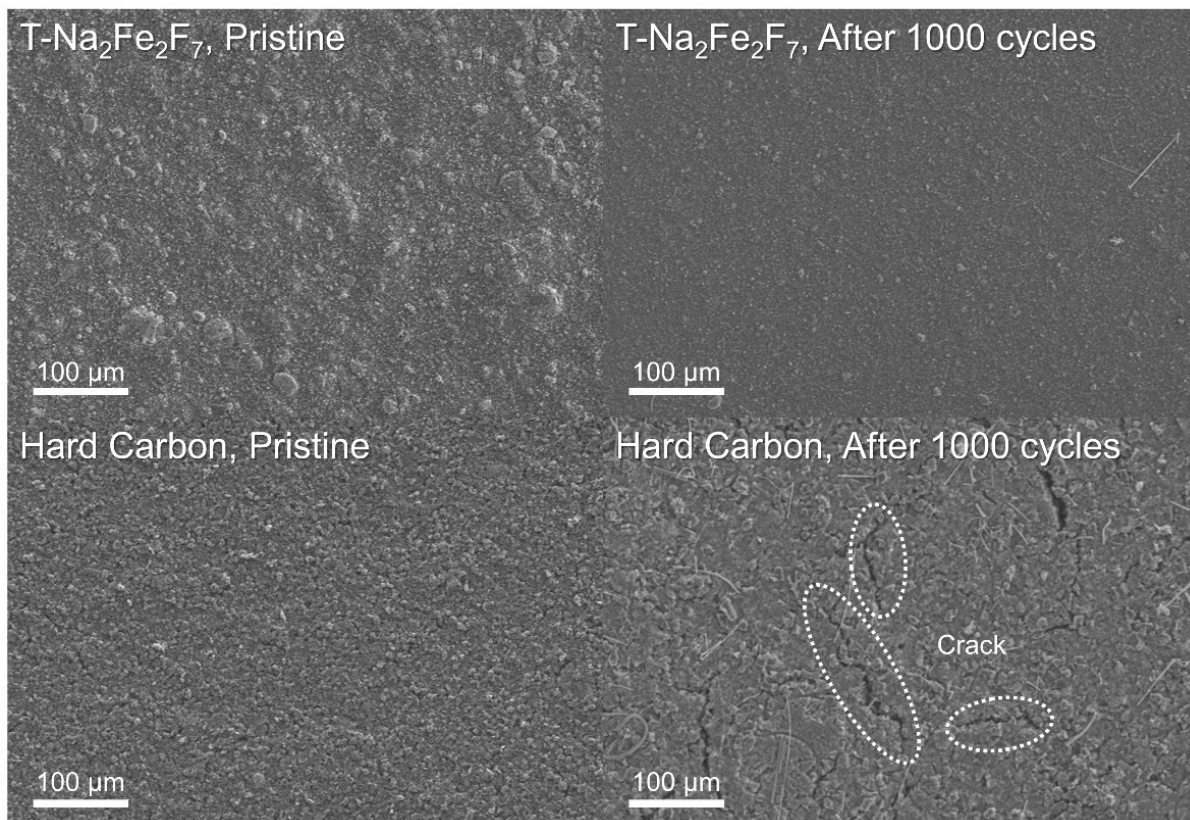


Fig. S13 SEM images of T-Na_xFe₂F₇ and hard carbon electrode after cycling for 1000 cycles.

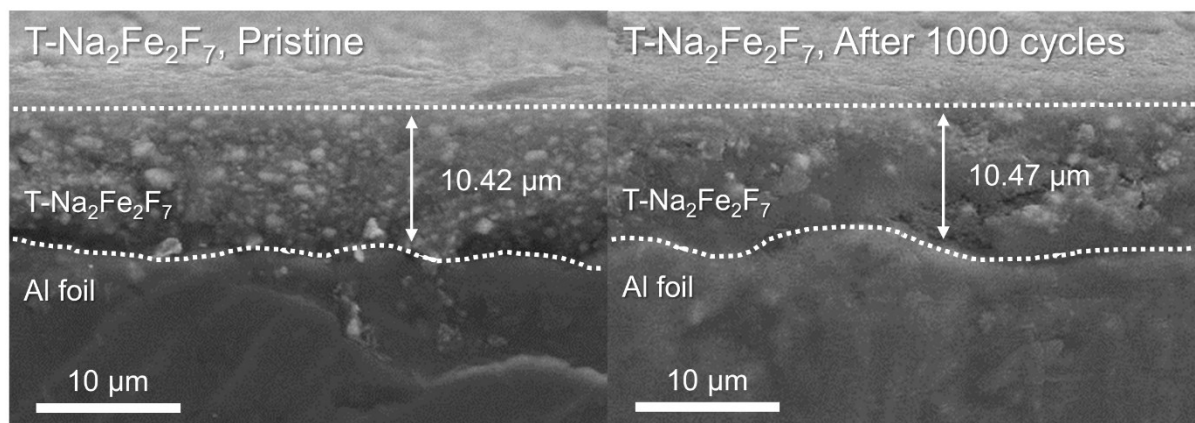


Fig. S14 Cross-SEM images of T-Na_xFe₂F₇ electrode before and after cycling for 1000 cycles.

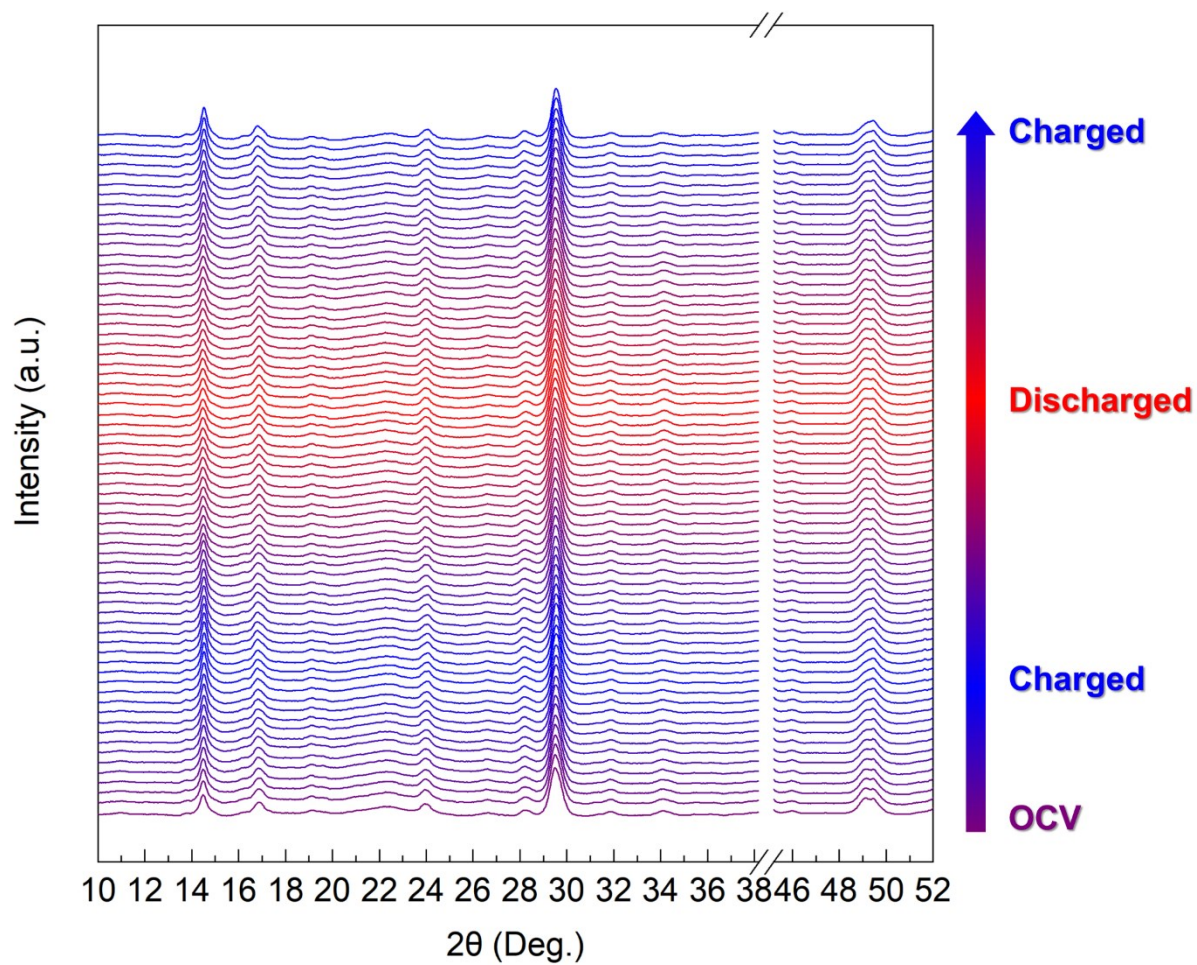


Fig. S15 Full *operando* Synchrotron XRD patterns of T-Na₂Fe₂F₇.

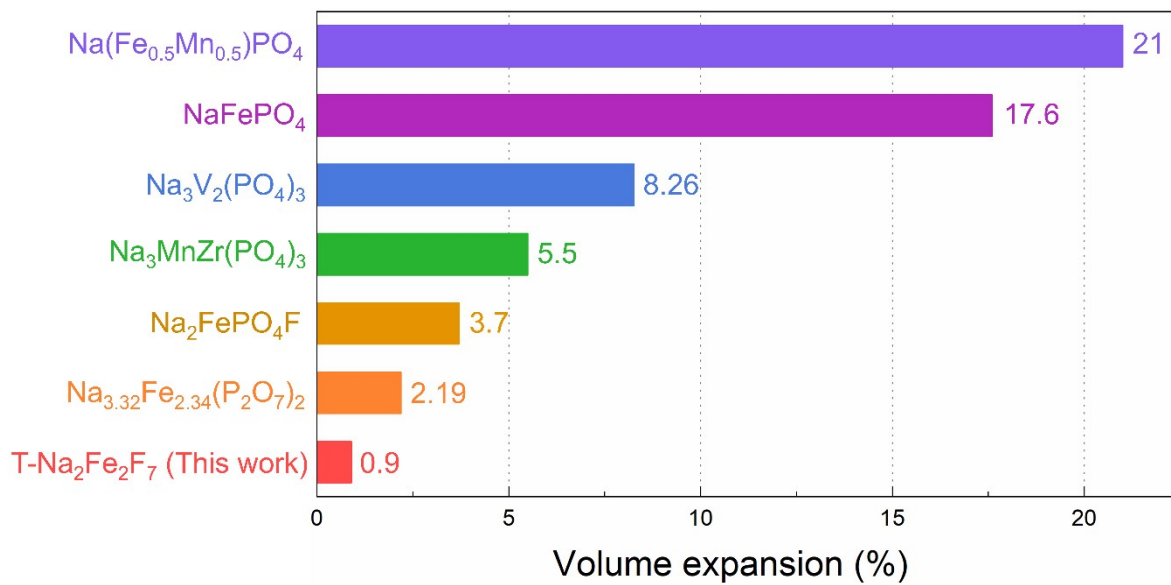


Fig. S16 Comparison of volume expansion of T- $\text{Na}_2\text{Fe}_2\text{F}_7$ and other cathode materials for NIBs.

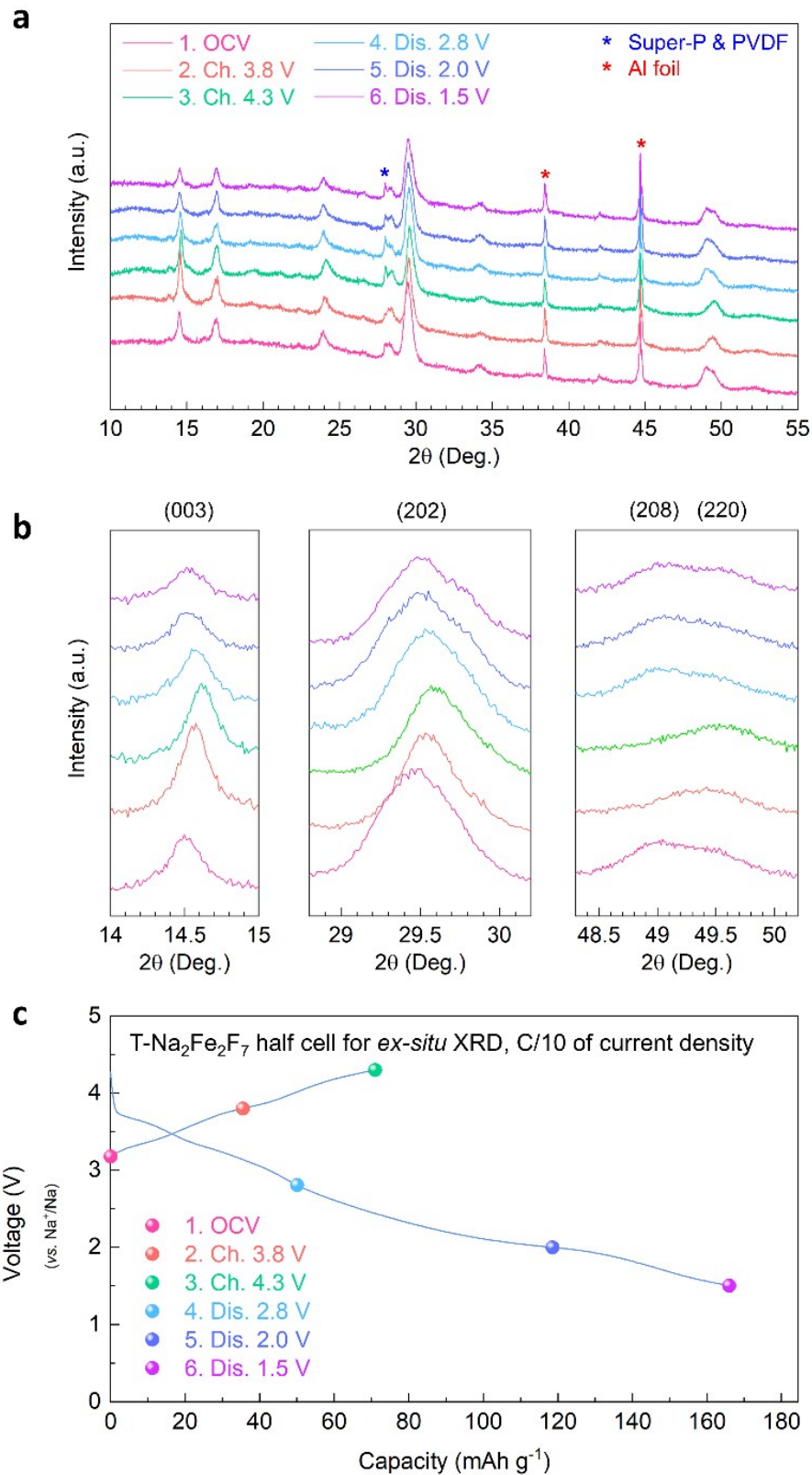


Fig. S17 (a and b) (a) *Ex-situ* patterns and (b) its magnified views of $\text{T-Na}_x\text{Fe}_2\text{F}_7$ ($1 \leq x \leq 3$).

(c) Charge/discharge profile of $\text{T-Na}_2\text{Fe}_2\text{F}_7$ for *ex-situ* XRD.

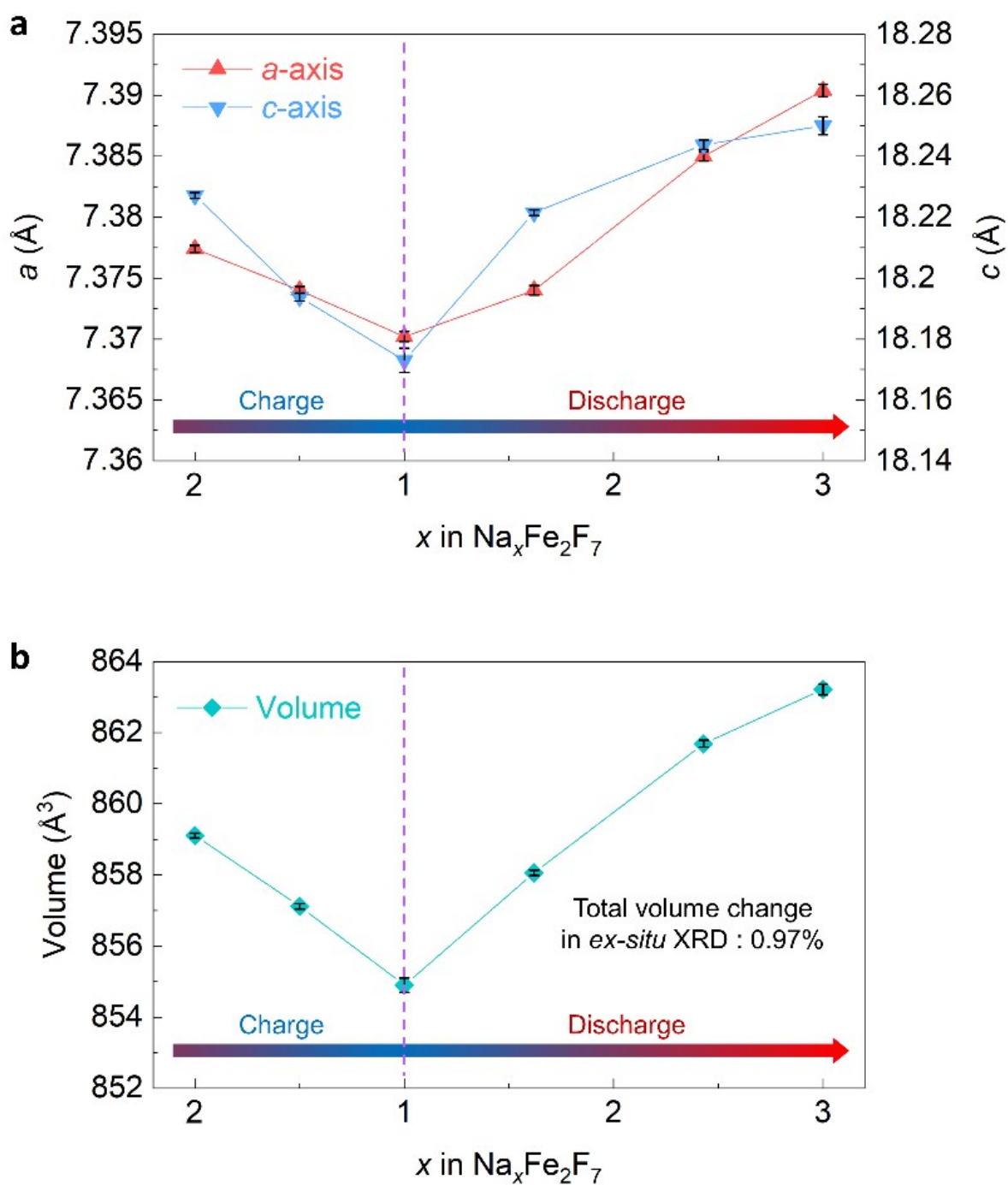


Fig. S18 (a and b) Change in (a) lattice parameter and (b) volume as a function of Na content in $\text{T-Na}_x\text{Fe}_2\text{F}_7$ ($1 \leq x \leq 3$) verified through Rietveld refinement based on *ex-situ* XRD patterns.

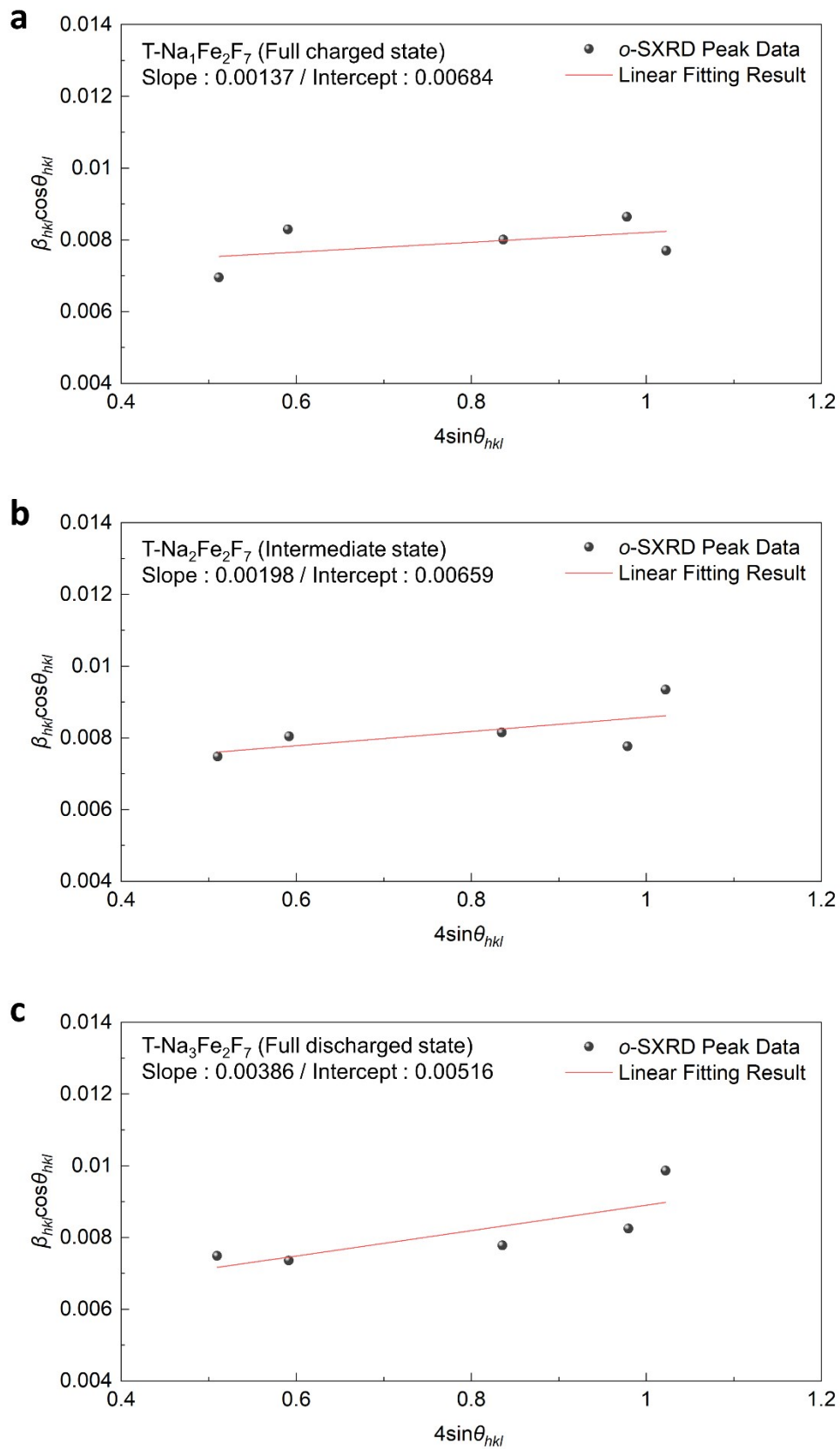


Fig. S19 W–H–ISM plot of T-Na_xFe₂F₇ based on *o*-SXR patterns ($1 \leq x \leq 3$).

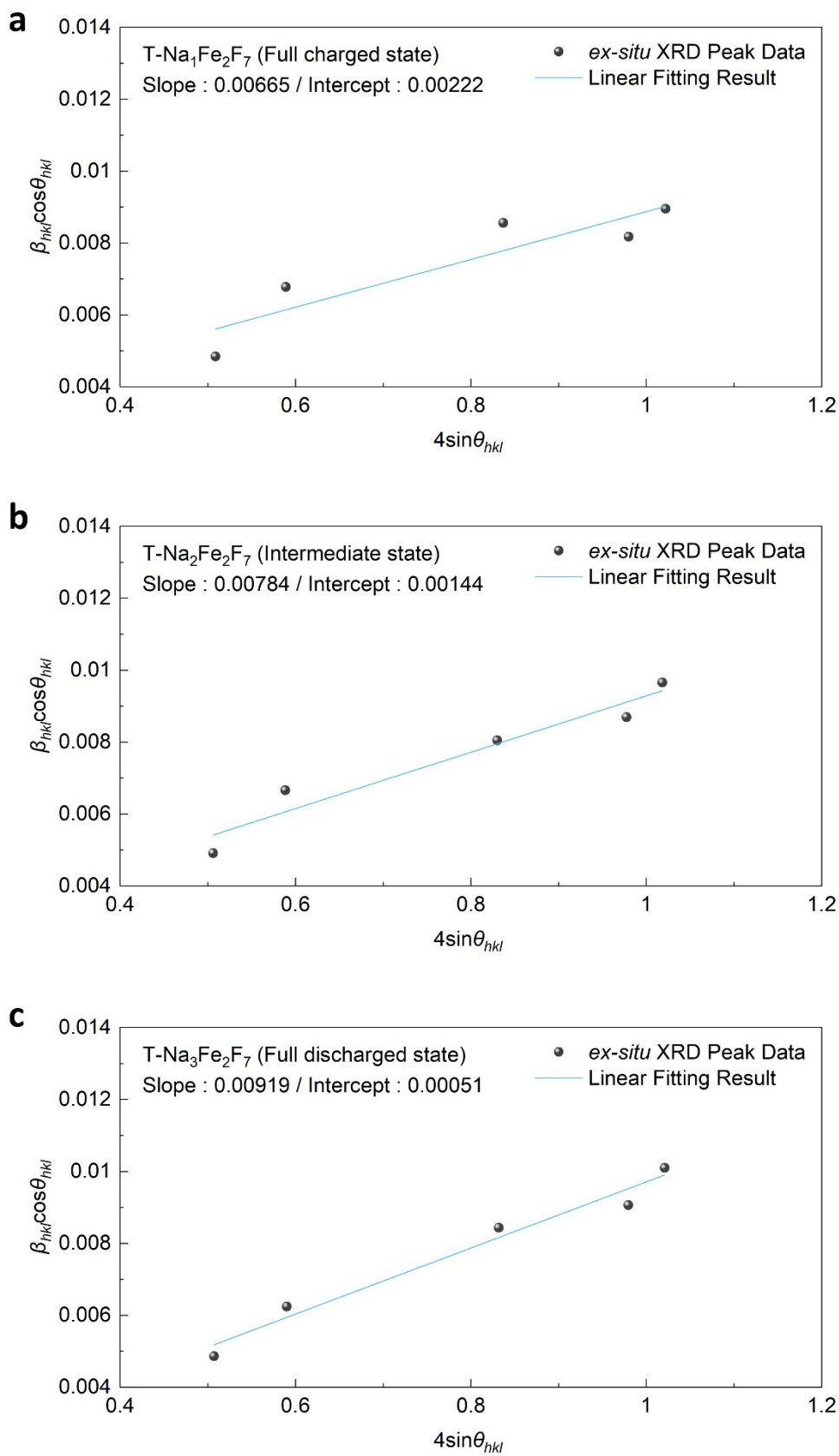
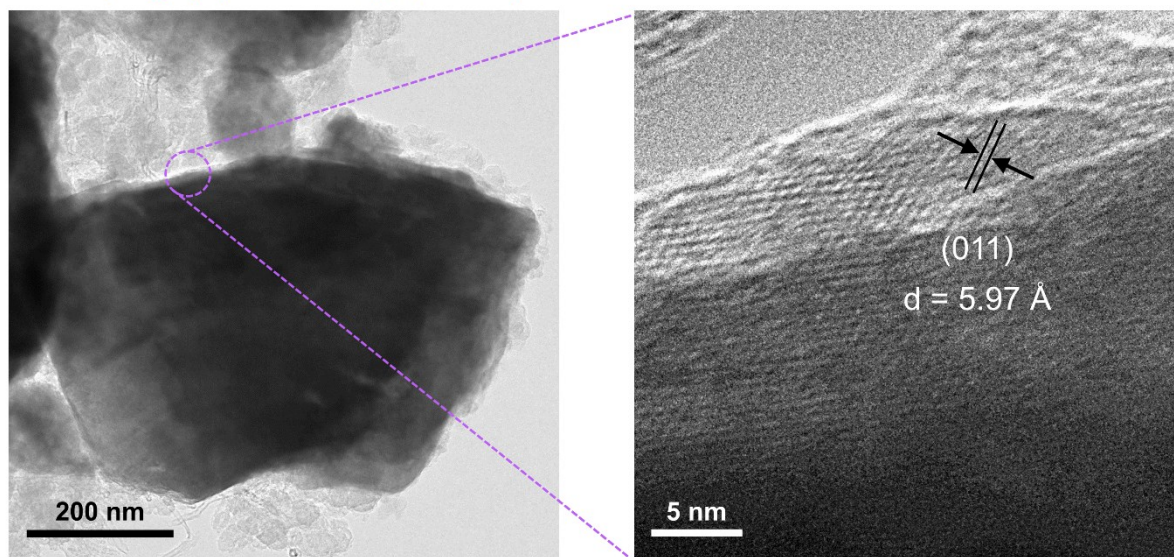


Fig. S20 W-H-ISM plot of T- $\text{Na}_x\text{Fe}_2\text{F}_7$ based on *ex-situ* XRD patterns ($1 \leq x \leq 3$).

T-Na₁Fe₂F₇ (Full Charge; 4.3 V)



T-Na₃Fe₂F₇ (Full Discharge; 1.5 V)

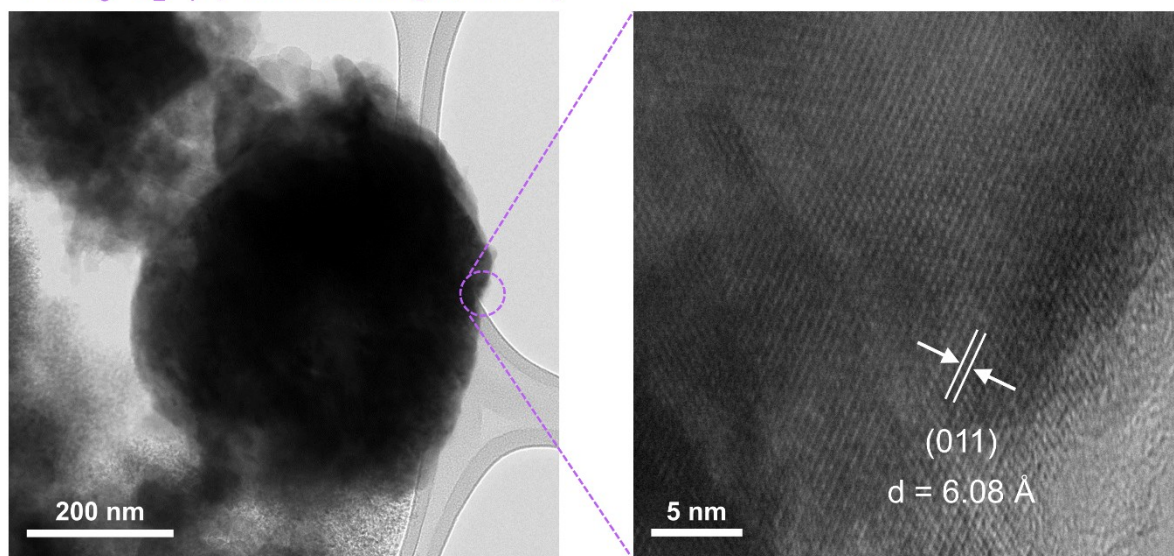


Fig. S21 TEM image with magnified view of T-Na₁Fe₂F₇ and T-Na₃Fe₂F₇.

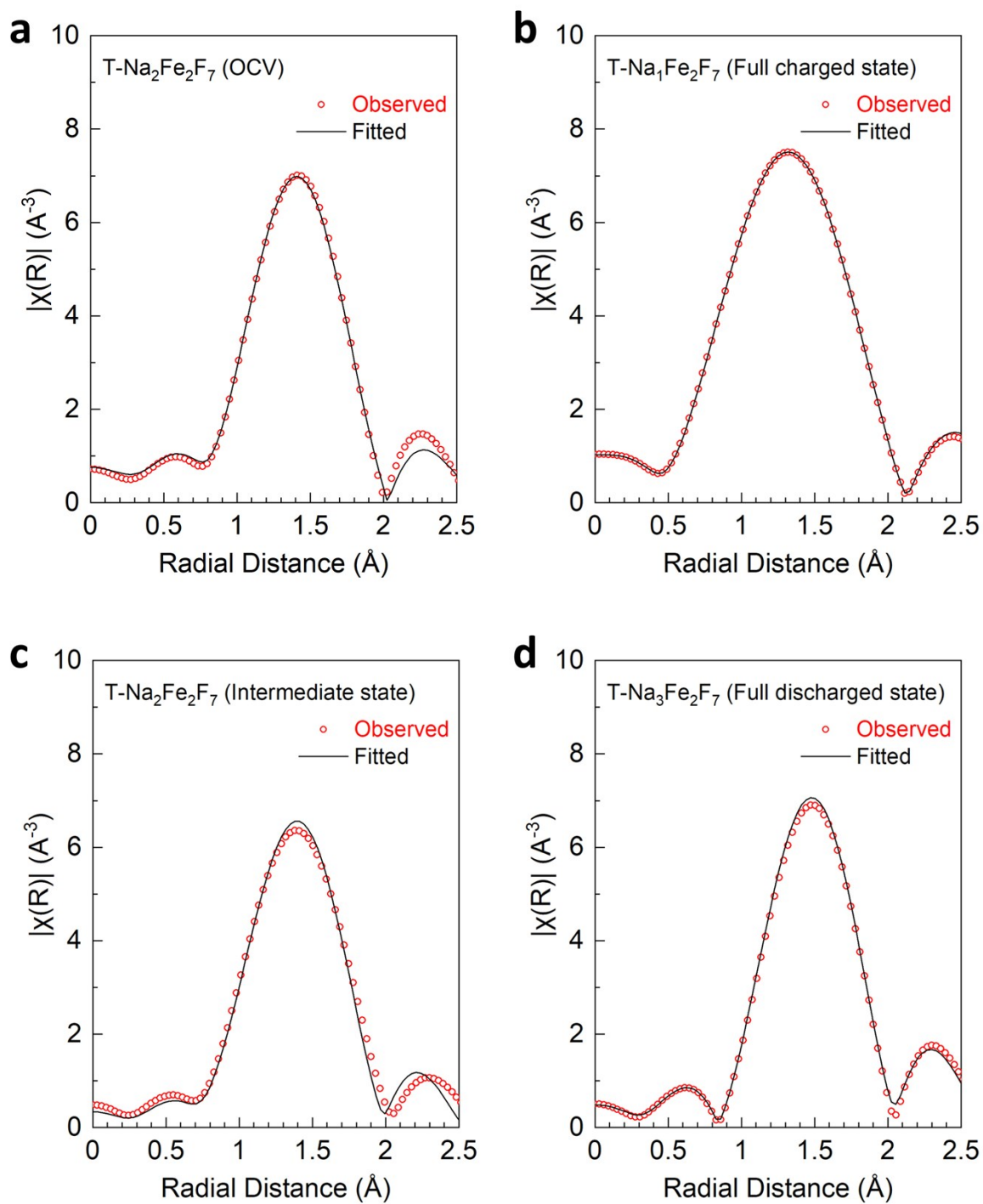


Fig. S22 EXAFS fits to data of $T\text{-Na}_x\text{Fe}_2\text{F}_7$ ($1 \leq x \leq 3$).

Supplementary Tables

| | Na | Fe |
|--|-------|-------|
| Na ₂ Fe ₂ F ₇ | 1.988 | 2.000 |

Table S1 ICP-OES results for T-Na₂Fe₂F₇.

Crystal structure : Trigonal

Space Group : $P\bar{3}_1 2 1$ (152)

Lattice parameters : $a = b = 7.3774(3)$, $c = 18.2288(12)$

| Atom | Wyckoff position | x | y | z | B _{iso} | Occupancy |
|------|------------------|-----------|----------|------------|------------------|-----------|
| Fe1 | 3a | 0.337(2) | 0 | 0.33333 | 1.97(5) | 1 |
| Fe2 | 3b | 0.337(3) | 0 | 0.83333 | 1.97(5) | 1 |
| Fe3 | 6c | 0.480(3) | 0.842(3) | 0.1688(9) | 1.97(5) | 1 |
| Na1 | 6c | 0.523(4) | 0.849(7) | 0.6653(16) | 0.33(20) | 1 |
| Na2 | 6c | 0.949(7) | 0.186(3) | 0.3357(19) | 0.33(20) | 0.5 |
| Na3 | 6c | 0.902(10) | 0.169(5) | 0.8626(20) | 0.33(20) | 0.5 |
| F1 | 6c | 0.754(5) | 0.203(9) | 0.601(2) | 1.75(9) | 1 |
| F2 | 6c | 0.798(7) | 0.965(5) | 0.9487(14) | 1.75(9) | 1 |
| F3 | 6c | 0.566(8) | 0.413(5) | 0.0544(15) | 1.75(9) | 1 |
| F4 | 6c | 0.831(7) | 0.452(9) | 0.187(2) | 1.75(9) | 1 |
| F5 | 6c | 0.048(5) | 0.334(6) | 0.2729(15) | 1.75(9) | 1 |
| F6 | 6c | 0.224(5) | 0.230(7) | 0.1460(18) | 1.75(9) | 1 |
| F7 | 6c | 0.066(7) | 0.444(5) | 0.8546(12) | 1.75(9) | 1 |

Table S2 Detailed structural information of T-Na₂Fe₂F₇ verified through Rietveld refinement.

| Active Materials | | Electrolyte | Voltage Range (V) | Cycle Retention (%) | Experimental condition | Ref. (in the main manuscript) |
|------------------|---|--|-------------------|---------------------|--|-------------------------------|
| Fluoride | T-Na ₂ Fe ₂ F ₇ | 0.5 M NaPF ₆ in PC:FEC (98:2 v/v%) | 1.5-4.3 | 88.3 | 1000 cycles at 368 mAh g ⁻¹ | This work |
| Layered-oxide | P2-Na _{0.6} [Li _{0.2} Ni _{0.2} Mn _{0.6}]O ₂ | 0.5 M NaPF ₆ in PC | 2.0-4.6 | 93.8 | 100 cycles at 12mAh g ⁻¹ | 36 |
| | P2-Na _{0.66} Co _{0.22} Mn _{0.44} Ti _{0.34} O ₂ | 1.0 M NaClO ₄ in EC:DEC (1:1 v/v%) | 1.5-4.3 | 73.3 | 200 cycles at 177 mAh g ⁻¹ | 37 |
| | O3-NaNi _{0.4} Mn _{0.25} Ti _{0.3} Co _{0.05} O ₂ | 1.0 M NaClO ₄ in EC:DEC (1:1 v/v%) | 2.0-4.4 | 60.1 | 180 cycles at 100 mAh g ⁻¹ | 38 |
| | O3-Na[Ni _{0.65} Co _{0.08} Mn _{0.27}]O ₂ | 0.5 M NaPF ₆ in PC:FEC (98:2 v/v%) | 1.5-4.1 | 90.0 | 50 cycles at 75 mAh g ⁻¹ | 39 |
| Polyanion | Na ₄ MnCr(PO ₄) ₃ | 1.0 M NaClO ₄ in PC:FEC (9:1 v/v%) | 1.5-4.3 | 71.5 | 250 cycles at 200 mAh g ⁻¹ | 40 |
| | Na ₂ Fe ₂ (SO ₄) ₃ | 1.0 M NaClO ₄ in EC:PC:FEC (1:1:0.05 v/v%) | 1.9-4.3 | 80.1 | 800 cycles at 600 mAh g ⁻¹ | 41 |
| | Na ₂ FePO ₄ F | 1.0 M NaPF ₆ in EC:PC (1:1 v/v) | 2.0-4.2 | 70.0 | 700 cycles at 124 mAh g ⁻¹ | 42 |
| | Na ₄ Mn ₃ (PO ₄) ₂ (P ₂ O ₇) | 1.0 M NaBF ₄ in EC:PC (1:1 v/v%) | 1.7-4.5 | 70.0 | 200 cycles at 130 mAh g ⁻¹ | 43 |
| Prussian-blue | Na ₂ Mn _{0.15} Co _{0.15} Ni _{0.1} Fe _{0.6} Fe(CN) ₆ | 1.0 M NaClO ₄ in EC:DEC:FEC (1:1:0.08 v/v%) | 2.0-4.0 | 81.1 | 500 cycles at 170 mAh g ⁻¹ | 44 |
| | Na ₂ CoFe(CN) ₆ | 1.0 M NaClO ₄ in EC:DEC (1:1 v/v%) | 2.0-4.1 | 89.1 | 200 cycles at 100 mAh g ⁻¹ | 45 |

Table S3 Electrochemical properties of various cathode materials for NIBs.

| <i>o</i> -SXR patterns | Lattice strain (ϵ) |
|--|-------------------------------|
| Na ₁ Fe ₂ F ₇ (Full charged state) | 0.00145 |
| Na ₂ Fe ₂ F ₇ (Intermediate state) | 0.00198 |
| Na ₃ Fe ₂ F ₇ (Full discharged state) | 0.00386 |

Table S4 Calculated lattice strain of Na_{*x*}Fe₂F₇ based on *o*-SXR patterns ($1 \leq x \leq 3$).

| <i>ex-situ</i> XRD patterns | Lattice strain (ϵ) |
|--|-------------------------------|
| Na ₁ Fe ₂ F ₇ (Full charged state) | 0.00665 |
| Na ₂ Fe ₂ F ₇ (Intermediate state) | 0.00784 |
| Na ₃ Fe ₂ F ₇ (Full discharged state) | 0.00919 |

Table S5 Calculated lattice strain of Na_xFe₂F₇ based on *ex-situ* XRD patterns ($1 \leq x \leq 3$).

| EXAFS data | Fe-F(1) | | Fe-F(2) | | Fe-F(3) | | χ^2 |
|--|---------------------------|------------------------------|---------------------------|------------------------------|---------------------------|------------------------------|----------|
| | (Coordination number : 2) | | (Coordination number : 2) | | (Coordination number : 2) | | |
| | d (Å) | σ^2 (Å ²) | d (Å) | σ^2 (Å ²) | d (Å) | σ^2 (Å ²) | |
| Na ₂ Fe ₂ F ₇ (OCV) | 1.964(7) | 0.0022(2) | 1.945(9) | 0.007(2) | 2.156(15) | 0.010(3) | 90.4 |
| Na ₁ Fe ₂ F ₇ (Full charged state) | 1.828(14) | 0.005(2) | 1.916(1) | 0.0004(1) | 2.031(14) | 0.008(3) | 98.8 |
| Na ₂ Fe ₂ F ₇ (Intermediate state) | 1.960(12) | 0.005(2) | 1.954(11) | 0.005(2) | 2.154(20) | 0.009(3) | 92.0 |
| Na ₃ Fe ₂ F ₇ (Full discharged state) | 2.042(1) | 0.004(1) | 2.011(10) | 0.005(1) | 2.329(15) | 0.007(3) | 95.2 |

Table S6 EXAFS fitting parameters for the first shell of T-Na_xFe₂F₇ ($1 \leq x \leq 3$).

References

- 1 H. Che, S. Chen, Y. Xie, H. Wang, K. Amine, X. Z. Liao and Z. F. Ma, *Energy Environ. Sci.*, 2017, **10**, 1075–1101.
- 2 S. Komaba, W. Murata, T. Ishikawa, N. Yabuuchi, T. Ozeki, T. Nakayama, A. Ogata, K. Gotoh and K. Fujiwara, *Adv. Funct. Mater.*, 2011, **21**, 3859–3867.
- 3 Y. J. Park, J. U. Choi, J. H. Jo, C. Jo, J. Kim and S. Myung, *Adv. Funct. Mater.*, 2019, **29**, 1901912.
- 4 L. Mu, M. M. Rahman, Y. Zhang, X. Feng, X. W. Du, D. Nordlund and F. Lin, *J. Mater. Chem. A*, 2018, **6**, 2758–2766.
- 5 E. de la Llave, V. Borgel, K.-J. Park, J.-Y. Hwang, Y.-K. Sun, P. Hartmann, F. F. Chesneau and D. Aurbach, *ACS Appl. Mater. Interfaces*, 2016, **8**, 1867–1875.
- 6 E. De La Llave, P. K. Nayak, E. Levi, T. R. Penki, S. Bublil, P. Hartmann, F. F. Chesneau, M. Greenstein, L. F. Nazar and D. Aurbach, *J. Mater. Chem. A*, 2017, **5**, 5858–5864.
- 7 J. Rodríguez-Carvajal, *Comm. powder Diffr. (IUCr). Newsl.*, 2001, **26**, 12–19.
- 8 B. Ravel and M. Newville, *J. Synchrotron Radiat.*, 2005, **12**, 537–541.
- 9 G. Kresse and J. Furthmüller, *Comput. Mater. Sci.*, 1996, **6**, 15–50.
- 10 P. E. Blöchl, *Phys. Rev. B*, 1994, **50**, 17953–17979.
- 11 J. P. Perdew, K. Burke and M. Ernzerhof, *Phys. Rev. Lett.*, 1996, **77**, 3865–3868.
- 12 V. I. Anisimov, F. Aryasetiawan and A. I. Lichtenstein, *J. Phys. Condens. Matter*,

- 1997, **9**, 767–808.
- 13 R. F. Li, S. Q. Wu, Y. Yang and Z. Z. Zhu, *J. Phys. Chem. C*, 2010, **114**, 16813–16817.
 - 14 Z. Li, B. Wang, C. Li, J. Liu and W. Zhang, *J. Mater. Chem. A*, 2015, **3**, 16222–16228.
 - 15 G. Henkelman, B. P. Uberuaga and H. Jónsson, *J. Chem. Phys.*, 2000, **113**, 9901–9904.
 - 16 K. Momma and F. Izumi, *J. Appl. Crystallogr.*, 2008, **41**, 653–658.